Available online at www.sciencedirect.com
ScienceDirect
Inorganica Chimica Acta 360 (2007) 1961–1969
Inorganica Chimica Acta
www.elsevier.com/locate/ica

Synthesis and characterization of heteroscorpionate dioxo-tungsten(VI) complexes

Ba L. Tran, Carl J. Carrano *

Department of Chemistry and Biochemistry, San Diego State University, San Diego, CA 92182-1030, USA

Received 12 September 2006; accepted 14 October 2006
Available online 10 November 2006

Abstract

Twelve new dioxo W(VI) complexes of a family of heteroscorpionate ligands of the type [(L)WO_2Y], where L = N_2X ligand and Y = Cl or OR, have been synthesized and characterized. With the more sterically bulky ligands we show that these complexes exist as isolable *cis* and *trans* isomers and compare the rate of such isomerization with their corresponding dioxo Mo(VI) analogs.
© 2006 Elsevier B.V. All rights reserved.

Keywords: Tungsten complexes; Heteroscorpionate ligands; X-ray diffraction

1. Introduction

Oxygen atom transfer (OAT) reactions between closed shell molecules are an important class of transformations that are catalyzed by a number of oxo metal complexes. Of particular interest have been catalysts derived from Re, Mo, and W. The first because of their extraordinary catalytic efficiency in carrying out even difficult oxygen atom transfers such as the conversion of ClO_4^- to Cl^- and the latter because of their potential biological relevance [1–3]. Thus there are a large number of mononuclear molybdenum and tungsten containing enzymes that have the general function of catalyzing OAT to or from a physiological donor/acceptor with the metal cycling between the +6 and +4 oxidation states.

Tripodal pyrazolylborate (Tp^R) and pyrazolylmethane complexes of molybdenum and tungsten represent a uniquely successful and extensive model system for the pterin dependent molybdo- and tungstoenzymes as well as a platform for Re based OAT catalysts [4–12]. While in general one would suppose that a threefold symmetric, all nitrogen donor ligand would be a poor substitute for the dithiolene and other sulfur donor atoms typical of molybdo and tungstoenzymes, they nevertheless provide biomimetic attributes unmatched by any other system. Over the last several years we and others have developed a series of polyfunctional, facially coordinating, tridentate ligands containing two pyrazole groups, which also incorporate another coordinating moiety (thiolate, phenolate, alkoxide, carboxylate, etc.) to produce various heteroscorpionate ligands with the same topology and charge as Tp^R [13–15]. Molybdenum complexes of these ligands of the type [(L)MoO_nCl_z] (where L = N_2X ligand) proved to be easily accessible and were shown to exist in two isomeric forms with the X donor atom *cis* or *trans* relative to an oxo group [16–18]. The two isomers differ significantly in their physiochemical properties. Mass spectrometry, DFT calculations and detailed kinetic analysis suggest that the isomerization of [(L)MoO_nCl_z] proceeds through a ''trigonal twist'' mechanism, the rate and equilibrium isomer ratio of which, are controlled by both electronic and steric factors. Although not explicitly invoked in the mechanism of action of any molybdo or tungstoenzyme, there is

* Corresponding author. Tel.: +1 619 594 5929; fax: +1 619 594 4634.
E-mail address: carrano@sciences.sdsu.edu (C.J. Carrano).

0020-1693/$ - see front matter © 2006 Elsevier B.V. All rights reserved.
doi:10.1016/j.ica.2006.10.024

evidence that conformational changes at the metal center could be occurring during the redox cycle [19–21]. Such processes have also been suggested by detailed studies of

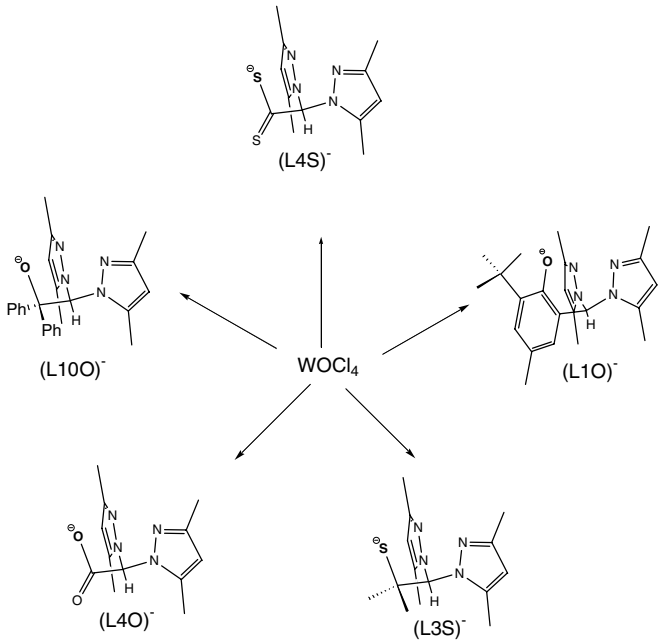

the mechanism of OAT catalyzed by small molecule complexes of Mo and Re [22,23]. Thus in addition to the ability to change donor atoms at will, a major advantage of the unsymmetrical N_2X heteroscorpionate ligands is their potential to explore the effects of geometry on OAT reactions. In this report we show that dioxo W(VI) complexes of heteroscorpionate ligands also exist as isolable *cis* and *trans* isomers and we compare the rate of such isomerization with the corresponding dioxo Mo(VI) analogs.

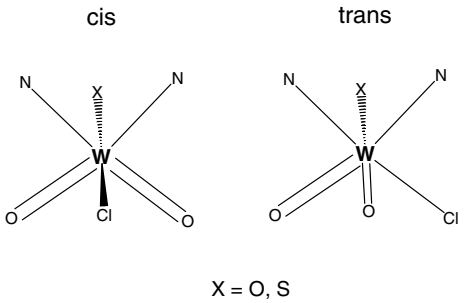

2. Experimental

All syntheses were initially carried out under inert nitrogen atmosphere using standard Schlenk or drybox techniques, but subsequent workups were conducted in air. The reagents, solvents, silica gel 60–200 mesh used in adsorption chromatography, and filtering agent Celite, were purchased from the Aldrich Chemical Co. and used as received unless otherwise noted. The ligands (L4S)Li, (L4O)Li, L1OH, L10OH, and L3SH were prepared using previously reported procedures [24]. The tungsten precursor $WO_2(acac)_2$ was synthesized following procedure published by Holm [25]. $WOCl_4$ is commercially available or synthesized via a literature method [26].

*[(L1O)WO_2Cl] (**1**)* . A mixture of L1OH (526 mg, 1.40 mmol) and NaOMe (78 mg, 1.44 mmol) were stirred in THF for 0.5 h. The resulting deprotonated ligand was added via cannula to a solution of $WOCl_4$ (465 mg, 1.36 mmol) in 50 mL of THF under nitrogen at RT. Upon addition of the ligand the solution turned an intense brown color and was stirred for 20 h. After removing THF, the mixture was chromatographed on silica gel with dichloromethane as eluant. The resulting pale violet and yellow bands were collected and dried. The yellow solid was assigned as the *cis* isomer and the violet as the *trans* based on the proton NMR. Combined yield: 74%. *Anal.* Calc. for $C_{23}H_{31}ClWN_4O_3 \cdot CH_2Cl_2$: C, 39.37; H, 4.45; N, 7.98. Found: C, 38.49; H, 4.59; N, 8.18%. Symmetric isomer (*cis*): FTIR (KBr, cm^{-1}): *v* 907, 947 (W=O) cm^{-1}. ^1H NMR (d_6-acetone): δ 1.32 (s, 9H, –C(CH_3)$_3$), 2.26 (s, 3H, Ar–CH_3), 2.65 (s, 6H, Pz–CH_3), 2.67 (2, 6H, Pz–CH_3), 6.23 (s, 2H, Pz–*H*), 7.23 (s, 1H, Ar–*H*), 7.30 (s, 1H, –C*H*–C), 7.42 (s, 1H, Ar–*H*). Asymmetric isomer (*trans*): FTIR (KBr, cm^{-1}): *v* 866, 967 (*W*=O) cm^{-1}. ^1H NMR ($CDCl_3$) δ 1.41 (s, 9H, –C(CH_3)$_3$), 2.29 (s, 3H, Pz–CH_3), 2.33 (2, 3H, Pz–CH_3), 2.50 (s, 3H, Ar–CH_3), 2.71 (s, 3H, Pz–CH_3), 2.73 (s, 3H, Pz–CH_3), 6.00 (s, 1H, Pz–*H*), 6.08 (s, 1H, Pz–*H*), 6.97 (s, 1H, –C*H*–C), 7.18 (s, 1H, Ar–*H*), (s, 1H, –C*H*–C), 7.22 (s, 1H, Ar–*H*).

*[(L10O)WO_2Cl] (**2**)*. A solution of L10OH (255 mg, 0.66 mmol) and NaOMe (36 mg, 0.67 mmol) was stirred in 20 mL THF for 0.5 h. The deprotonated ligand was then added dropwise via syringe to a solution of $WOCl_4$ (225 mg, 0.66 mmol) in 30 mL of THF under nitrogen at RT. The solution immediately decolorized and after stirring for 20 h was filtered through Celite to remove NaCl and blue insoluble solids. Concentrating the filtrate to dryness afforded a cream colored solid. Recrystallization was from dichloromethane/hexane. Yield: 76%. *Anal.* Calc. for $C_{24}H_{25}ClWN_4O_3$: C, 45.27; H, 3.96; N, 8.80. Found: C, 45.12; H, 3.80; N, 8.62%. Symmetric isomer (*cis*): FTIR (KBr, cm^{-1}): *v* 947, 903 (W=O) cm^{-1}. ^1H NMR ($CDCl_3$) δ 7.51–755 (m, 5H, Ar–*H*), 7.23–7.27 (m, 5H, Ar–*H*), 6.76 (s, 1H, –C*H*C–), 5.82 (s, 2H, Pz–*H*), 2.61 (s, 6H, Pz–CH_3), 2.20 (s, 6H, Pz–CH_3). ^{13}C NMR (DMSO) δ 157.78, 143.18, 128,83, 126.39, 108.19, 98.55, 88.69, 82.69, 28.51, 14.15, 11.51. Asymmetric isomer (*trans*): ^1H NMR ($CDCl_3$) δ 7.63–7.78 (m, 5H, Ar–*H*), 7.18–7.21 (m, 5H, Ar–*H*), 6.81 (s, 1H, –C*H*–), 5.85 (s, 1H, Pz–*H*), 5.78 (s, 1H, Pz–*H*), 2.65 (s, 3H, Pz–CH_3), 2.58 (s, 3H, Pz–CH_3), 2.42 (s, 3H, Pz–CH_3), 2.25 (s, 3H, Pz–CH_3).

*[(L4O)WO_2Cl] (**3**)*. A solution of (L4O)Li (254 mg, 1.00 mmol) in 60 ml THF was added to via syringe to

$WOCl_4$ (338 mg, 0.99 mmol) dissolved in 20 mL of THF under nitrogen at RT. The solution decolorized and after stirring for 20 h a white solid was collected by filtration. Yield: 52%. *Anal.* Calc. for $C_{12}H_{15}N_4O_4ClW \cdot CHCl_3$: C, 25.26; H, 2.61; N, 9.07. Found: C, 25.20; H, 2.60; N, 9.51%. FTIR (KBr, cm^{-1}): *v* 911, 946 (W=O) cm^{-1}. ^1H NMR ($CDCl_3$): δ 2.08 (s, 3H, Pz–CH_3), 2.11 (s, 3H, Pz–CH_3), 2.17 (s, 3H, Pz–CH_3), 2.21 (s, 3H, Pz–CH_3), 5.89 (s, 1H, Pz–*H*), 6.38 (s, 1H, –C*H*–C), 7.14 (s, 1H, Pz–*H*).

*[(L3S)WO_2Cl] (**4**)*. A mixture of L3SH (250 mg, 0.89 mmol) and NaOMe (50 mg, 0.93 mmol) were stirred in 20 mL THF for 0.5 h. The resulting deprotonated ligand was added via syringe to a solution of $WOCl_4$ (307 mg, 0.89 mmol) in 25 mL of THF under nitrogen at RT. After stirring overnight, the reaction was vacuum filtered through a glass frit and the filtrate concentrate. Recrystallization from dichloromethane and pentane gave yellow solids. Yield: 32%. FTIR (KBr, cm^{-1}): *v* 907, 952 (W=O) cm^{-1}. ^1H NMR (DMSO): δ 1.22 (s, 6H, –C(CH_3)$_2$–), 2.30 (s, 3H, Pz–CH_3), 2.56 (s, 3H, Pz–CH_3), 5.82 (s, 2H, Pz–*H*), 6.33 (s, 1H, –C*H*–C). λ_{max} (CH_2Cl_2, ε, M^{-1} cm^{-1}): 370 (317), 395 (263).

Synthesis of [LWO_2(OR)]. Stoichiometric addition of ligand to a solution of $WO_2(acac)_2$ in ~50–70 mL of the appropriate alcohol followed by stirring at ambient temperature under a nitrogen atmosphere overnight resulted in precipitation of the desired products. The solid were collected by filtration and washed extensively with the appropriate alcohol followed by hexane and then dried under vacuum. Attempts to crystallize the alkoxy complexes at room temperature resulted in the formation of the corresponding μ-oxo dimers (these complexes were characterized only by X-ray crystallography of which [(L4O)-WO_2]$_2$O is presented as a representative example) rather than the expected mononuclear complexes. Therefore crystals of the mononuclear complexes suitable for X-ray diffraction were grown from dichloromethane/hexane at −20 °C.

*[(L1O)WO_2(OMe)] (**5**)*. L1OH (254 mg, 0.69 mmol) and $WO_2(acac)_2$ (281 mg, 0.68 mmol). The product is a white solid. Yield: 38%. *Anal.* Calc. for $C_{23}H_{324}O_4W \cdot CHCl_3$: C, 39.39; H, 4.54; N, 7.66. Found: C, 39.21; H, 4.08; N, 7.74%. FTIR (KBr, cm^{-1}): *v* 897, 941 vs (W=O) cm^{-1}. ^1H NMR ($CDCl_3$): δ 1.41 (s, 9H, –C(CH_3)$_3$), 2.28 (s, 3H, Ar–CH_3), 2.44 (s, 6H, Pz–CH_3), 2.63 (s, 6H, Pz–CH_3), 4.56 (s, 3H, –OCH_3), 5.98 (s, 2H, Pz–*H*), 6.82 (d, 1H, $J = 2$ Hz, Ar–*H*), 6.91 (s, 1H, –C*H*–C), 7.42 (d, 1H, $J = 2$ Hz, Ar–*H*). ^{13}C NMR ($CDCl_3$): δ 11.98, 14.73, 21.09, 30.62, 35.49, 66.61, 70.36, 108.55, 121.92, 126.95, 128.43, 130.66, 140.32, 143.12, 153.35, 157.59.

*[(L10O)WO_2(OMe)] (**6**)*. L10OH (255 mg, 0.66 mmol) and $WO_2(acac)_2$ (268 mg, 0.65 mmol). The product is a white solid. Yield: 52%. *Anal.* Calc. for $C_{25}H_{284}O_4W \cdot CHCl_3$: C, 41.54; H, 3.89; N, 7.45. Found: C, 41.95; H, 3.91; N, 7.63%. FTIR (KBr, cm^{-1}): *v* 892, 938 (W=O) cm^{-1}. ^1H NMR ($CDCl_3$): δ 2.17 (s, 6H, Pz–CH_3), 2.52 (s, 6H, Pz–CH_3), 4.60 (s, 3H, –OCH_3), 5.77 (s, 2H, Pz–*H*), 6.75 (s, 1H, –C*H*–C), 7.16–7.29 (m, 5H, Ar–*H*), 7.57–7.63 (m, 5H, Ar–*H*). ^{13}C NMR ($CDCl_3$): δ 8.00, 11.21, 14.15, 22.59, 51.15, 60.70, 71.69, 107.51, 126.29, 127.23, 128.07, 128.60, 139.97, 154.68.

*[(L4O)WO_2(OMe)] (**7**)*. L4OH (255 mg, 1.03 mmol) and $WO_2(acac)_2$ (418 mg, 1.01 mmol). The product is a white solid. Yield: 68%. *Anal.* Calc. for $C_{13}H_{18}N_4O_5W$: C, 31.60; H, 3.67; N, 11.34. Found: C, 31.55; H, 3.48; N, 11.53%. FTIR (KBr, cm^{-1}): *v* 915, 940 (W=O) cm^{-1}. ^1H NMR (DMSO): δ 2.48 (s, 3H, Pz–CH_3), 2.57 (s, 3H, Pz–CH_3), 2.63 (s, 3H, Pz–CH_3), 2.69 (s, 3H, Pz–CH_3), 5.86 (s, 3H, –OCH_3), 6.21 (s, 1H, Pz–*H*), 6.34 (s, 1H, Pz–*H*), 6.94 (s, 1H, –C*H*–C).

*[(L3S)WO_2(OMe)] (**8**)*. L3SH (254 mg, mmol) and $WO_2(acac)_2$ (mg, mmol). The product is an off-white solid. Yield: 70%. *Anal.* Calc. for $C_{15}H_{24}N_4O_3SW \cdot 3/4(CHCl_3)$: C, 30.81; H, 4.06; N, 9.13. Found: C, 30.54; H, 4.29; N, 9.31%. FTIR (KBr, cm^{-1}): *v* 896, 929 (W=O) cm^{-1}. ^1H NMR (DMSO): δ 1.21 (s, 6H, –C(CH_3)$_2$–), 2.10 (s, 3H, Pz–CH_3), 2.13 (s, 3H, Pz–CH_3), 3.72 (s, 3H, –OCH_3), 6.26 (s, 2H, Pz–*H*), 6.42 (s, 1H, –C*H*–C). λ_{max} (CH_2Cl_2, ε, M^{-1} cm^{-1}): 350 (293).

*[(L10O)WO_2(OPr^i)] (**9**)*. L10OH (255 mg, 0.66 mmol) and $WO_2(acac)_2$ (268 mg, 0.65 mmol). The product is a white solid. Yield: 62%. *Anal.* Calc. for $C_{27}H_{32}N_4O_4 \cdot H_2O$: C, 47.80; H, 5.05; N, 8.26. Found: C, 47.77; H, 4.45; N, 8.59%. FTIR (KBr, cm^{-1}): *v* 888, 928 (W=O) cm^{-1}. ^1H NMR ($CDCl_3$): δ 1.46 (s, 3H, –C(CH_3)$_2$), 1.49 (s, 3H, –C(CH_3)$_2$), 2.15 (s, 6H, Pz–CH_3), 2.54 (s, 6H, Pz–CH_3), 5.04 (m, 1H, –OC*H*–), 5.74 (s, 2H, Pz–*H*), 6.68 (s, 1H, –C*H*–C), 7.15–7.28 (m, 5H, Ar–*H*), 7.59–7.63 (m, 5H, Ar–*H*). ^{13}C NMR ($CDCl_3$): δ 11.34, 14.47, 25.48, 71.63, 80.04, 80.96, 107.28, 126.39, 127.93, 128.48, 139.92, 142.86, 152.06.

*[(L1O)WO_2(OPr^i)] (**10**)*. L1OH (254 mg, 0.69 mmol) and $WO_2(acac)_2$ (281 mg, 0.68 mmol). The product is a white solid. Yield: 48%. *Anal.* Calc. for $C_{25}H_{34}N_4O_4W \cdot 2H_2O$: C, 45.60; H, 5.81; N, 8.51. Found: C, 45.61; H, 5.21; N, 8.77%. FTIR (KBr, cm^{-1}): *v* 897, 941 (W=O) cm^{-1}. ^1H NMR ($CDCl_3$): δ 1.39 (s, 6H, –C(CH_3)$_2$), 1.42 (s, 9H, –C(CH_3)$_3$), 2.26 (s, 3H, Ar–CH_3), 2.45 (s, 6H, Pz–CH_3), 2.65 (s, 6H, Pz–CH_3), 5.00 (m, 1H, –OC*H*–), 5.96 (s, 2H, Pz–*H*), 6.79 (d, 1H, $J = 2$ Hz, Ar–*H*), 6.89 (s, 1H, –C*H*–C), 7.16 (d, 1H, $J = 2$ Hz, Ar–*H*). ^{13}C NMR ($CDCl_3$): δ 12.10, 15.00, 21.09, 25.26, 30.62, 35.46, 70.49, 81.72, 108.72, 108.37, 121.95, 126.77, 127.73, 130.50, 140.27, 143.09, 152.96, 157.94.

*[(L4S)WO_2(OPr^i)] (**11**)*. L4SH (254 mg, 0.90 mmol) and $WO_2(acac)_2$ (376 mg, 0.90 mmol). The product is a yellow solid. Yield: 60%. *Anal.* Calc. for $C_{15}H_{22}N_4O_3S_2W \cdot 7/4(CHCl_3)$: C, 26.36; H, 3.13; N, 7.34. Found: C, 26.62; H, 3.09; N, 6.60%. FTIR (KBr, cm^{-1}): *v* 904, 936 (W=O) cm^{-1}. ^1H NMR (DMSO): δ 1.30 (s, 6H, –C(CH_3)$_2$), 1.33 (s, 9H, –C(CH_3)$_3$), 2.08 (s, 6H, Pz–CH_3), 2.17 (s, 6H, Pz–CH_3), 5.69 (s, 2H, Pz–*H*), 5.84 (m, 1H, –OC*H*–) 6.86 (s, 1H, –C*H*–C).

Physical methods. Elemental analysis was performed at Numega Resonance Labs, Inc. (San Diego, CA). $^{1}H/^{13}C$ NMR spectra were recorded on a Varian FT-NMR spectrometer running at 200 or 500 MHz located in the Department of Chemistry and Biochemistry, San Diego State University. UV–Vis spectra were recorded using a Cary 50 UV–visibility spectrophotometer under PC control using the Cary WinUV software. Infrared spectra were collected KBr disks on a Thermo-Nicolet Nexus 670 FT-IR spectrometer under PC control and are reported in wavenumbers.

X-ray crystallography. Data collection and refinement parameters for [(L1O)WO_2Cl] (**1**), [(L10O)WO_2(OMe)] (**6**), and [(L4O)WO_2]$_2$O (**12**) are given in Table 1. The structures were solved by either direction methods or Patterson function, completed by subsequent difference Fourier syntheses, and refined by full-matrix least-squares procedures on F^2. All non-hydrogen atoms were refined with anisotropic displacement coefficients, while hydrogen atoms were treated as idealized contributions using a rigid model except where noted. Selected bond distances and angles for [(L1O)WO_2Cl] (**1**) and [(L10O)WO_2(OMe)] (**6**) are presented in Table 2 while those for **12** are given in Table 3.

3. Results and discussion

3.1. Synthesis and reactivity

Conventionally, dioxo-tungsten complexes are synthesized from WO_2Cl_2, $WO_2(acac)_2$, and more recently [WO_2Cl_2(dme)] (dme = 1,2-dimethoxyethane) as tungsten sources. The major difficulty with employing the chloride containing salt is its poor solubility in most organic solvents. Thus many have turned to the soluble [WO_2Cl_2(dme)] derivative as synthon [27]. However synthesis of this soluble tungsten derivative requires two synthetic steps starting from WCl_6 which after treatment with hexamethyldisiloxane (HMDO) generates the intermediate $WOCl_4$, which is again treated with HMDO and dimethoxyethane (dme) to give [WO_2Cl_2(dme)] [28]. Fortunately, we are able to employ $WOCl_4$ directly with N_2X ligands in dry THF at room temperature under nitrogen atmosphere to generate [LWO_2Cl] complexes

Table 1
Summary of crystallographic data and parameters for [(L1O)WO_2Cl] (**1**), [(L10O)WO_2(OMe)] (**6**), and [(L4O)WO_2]$_2$O (**12**)

	1	**6**	**12**
Molecular formula	$C_{22}H_{19}N_4O_3ClW$	$C_{25}H_{28}N_4O_4W$	$C_{24}H_{30}N_8O_9W_2$
F_w	616.78	632.16	942.26
Temperature (K)	220(2)	220(2)	220(2)
Crystal system	rhombohedral	orthorhombic	orthorhombic
Space group	*R*3*m*	$P2_12_12_1$	*Pbca*
Unit cell dimensions			
a (Å)	27.651(19)	9.303(4)	15.9542(15)
b (Å)	27.651(19)	15.035(6)	15.8568(16)
c (Å)	9.140(7)	19.560(8)	22.640(3)
α (°)	90	90	90
β (°)	90	90	90
γ (°)	120	90	90
Z	9	4	8
V (Å^3)	6052.0(7)	2736.0(2)	5727.4(10)
Absorption coefficient, δ_{calc} (mm^{-1})	4.430	4.456	8.094
δ_{calc} (g/cm^3)	1.597	1.741	2.185
F(000)	2862	1416	3600
Crystal dimension (mm)	0.2 × 0.2 × 0.1	0.4 × 0.4 × 0.3	0.3 × 0.2 × 0.1
Radiation	Mo Kα	Mo Kα	Mo Kα
λ (Å)	0.71073	0.71073	0.71073
h, *k*, *l* ranges collected	−38 → 38, −38→38, −12 → 11	−13 → 13, −20 → 22, −28 → 28	−22 → 22, −22 → 22, −31 → 32
θ Range (°)	2.55–30.03	2.42–31.51	2.55–30.58
Number of reflections collected	4039	8341	6542
Number of unique reflections	3514	9078	8732
Number of parameters	172	334	388
Data/parameter ratio	20.43	27.18	22.50
Refinement method	full-matrix least-squares of F^2	full-matrix least-squares of F^2	full-matrix least-squares of F^2
$R(F)$[a]	0.042	0.0235	0.0360
$R_w(F^2)$[b]	0.122	0.0585	0.0896
GOFw[c]	1.075	1.025	1.018
Largest difference in peak and hole (e/Å^3)	2.646 and −2.492	1.672 and −0.668	4.618 and −1.342

[a] $R=[|\delta F|/|F_o|]$.
[b] $R_w = [w(\delta F)^2/wF_o^2]$.
[c] Goodness-of-fit on F^2.

Table 2
Selected bond distances (Å) and angles (°), respectively, for [(L1O)WO_2Cl] (**1**), [(L10O)WO_2(OMe)] (**6**)

	1	**6**		**1**		**6**
W(1)–N(1)	2.341(7)	2.314(2)	O(1)–W(1)–O(1)	103.6(4)	O(2)–W(1)–O(1)	102.93(12)
W(1)–N(3)	2.341(7)	2.347(3)	O(1)–W(1)–O(2)	98.44(19)	O(2)–W(1)–O(3)	98.53(10)
W(1)–O(1)	1.788(5)	1.732(2)	O(1)–W(1)–N(1)	166.2(2)	O(1)–W(1)–O(3)	98.94(11)
W(1)–O(2)	1.788(5)	1.724(2)	O(1)–W(1)–N(1)	90.1(3)	O(2)–W(1)–O(4)	99.90(10)
W(1)–O(3)	1.910(6)	1.913(2)	O(2)–W(1)–N(1)	81.2(2)	O(1)–W(1)–O(4)	98.62(10)
W(1)–O(4)		1.938(2)	O(1)–W(1)–N(1)	90.1(2)	O(3)–W(1)–O(4)	150.92(8)
W(1)–Cl(1)	2.376(2)		O(1)–W(1)–N(1)	166.2(2)	O(2)–W(1)–N(1)	164.48(10)
			O(2)–W(1)–N(1)	81.2(2)	O(1)–W(1)–N(1)	92.59(10)
			N(1)–W(1)–N(1)	76.2(3)	O(3)–W(1)–N(1)	79.05(8)
			O(1)–W(1)–Cl(1)	94.50(16)	O(4)–W(1)–N(1)	77.16(8)
			O(1)–W(1)–Cl(1)	94.50(16)	O(2)–W(1)–N(3)	89.24(10)
			O(2)–W(1)–Cl(1)	159.0(2)	O(1)–W(1)–N(3)	167.72(10)
			N(1)–W(1)–Cl(1)	82.27(15)	O(3)–W(1)–N(3)	80.59(9)
					O(4)–W(1)–N(3)	77.37(8)
					N(1)–W(1)–N(3)	75.24(8)

Table 3
Selected bond distances (Å) and angles (°), respectively, for [(L4O)WO_2]$_2$O (**12**)

W(1)–O(2)	1.710(4)	O(2)–W(1)–O(1)	102.4(2)	O(6)–W(2)–O(5)	103.4(2)
W(1)–O(1)	1.717(4)	O(2)–W(1)–O(9)	101.85(19)	O(6)–W(2)–O(9)	103.04(19)
W(1)–O(9)	1.883(4)	O(1)–W(1)–O(9)	103.00(18)	O(5)–W(2)–O(9)	102.73(19)
W(1)–O(3)	2.099(4)	O(2)–W(1)–O(3)	93.30(19)	O(6)–W(2)–O(8)	160.86(17)
W(1)–N(1)	2.214(5)	O(1)–W(1)–O(3)	159.26(18)	O(5)–W(2)–O(8)	91.48(18)
W(1)–N(3)	2.361(4)	O(9)–W(1)–O(3)	86.60(16)	O(9)–W(2)–O(8)	84.93(16)
W(2)–O(6)	1.713(4)	O(2)–W(1)–N(1)	90.59(18)	O(6)–W(2)–N(7)	89.63(18)
W(2)–O(5)	1.718(4)	O(1)–W(1)–N(1)	89.28(18)	O(5)–W(2)–N(7)	89.37(18)
W(2)–O(9)	1.876(4)	O(9)–W(1)–N(1)	160.01(17)	O(9)–W(2)–N(7)	159.71(16)
W(2)–O(8)	2.149(4)	O(3)–W(1)–N(1)	77.02(16)	O(8)–W(2)–N(7)	78.46(15)
W(2)–N(7)	2.198(4)	O(2)–W(1)–N(3)	165.52(18)	O(6)–W(2)–N(5)	86.78(19)
W(2)–N(5)	2.332(4)	O(1)–W(1)–N(3)	86.31(18)	O(5)–W(2)–N(5)	162.43(18)
		O(9)–W(1)–N(3)	87.12(17)	O(9)–W(2)–N(5)	88.53(16)
		O(3)–W(1)–N(3)	75.73(15)	O(8)–W(2)–N(5)	75.93(15)
		N(1)–W(1)–N(3)	77.88(17)	N(7)–W(2)–N(5)	76.27(16)

(L = L1O$^-$, L10O$^-$, L4O$^-$, L3S$^-$) thereby saving a synthetic step. When the orange solid $WOCl_4$ was treated with THF a reaction occurs immediately to generate a canary yellow precipitate. The additional oxo group found in the products undoubtedly results from the tungsten oxytetrachloride abstracting an oxygen atom from solvent THF to form $WO_2Cl_2(THF)_2$ in situ. All heteroscorpionate mononuclear dioxo W(VI) chloro complexes isolated are air stable and range in color from white to yellow. Most are soluble in common organic solvents such as dichloromethane, chloroform, acetonitrile, and dimethyl sulfoxide. Use of the sterically encumbered L1OH and L10OH ligands to form [(L)WO_2Cl] complexes, produced both *cis* and *trans* isomers which were easily recognized by NMR spectroscopy based on the behavior of the pyrazole proton. Lehtonen and co-workers have also reported the presence of isomers for mononuclear $LWOCl_2$ type complexes, in which the ligand was an NO_2 Schiff base [29].

In addition to the chloro complexes we have also synthesized a range of alkoxide substituted [LWO_2OR] species where R = Me, Pr^i. The reaction between the protonated scorpionate ligands and $WO_2(acac)_2$ in methanol or isopropanol directly precipitated the desired complexes. The presence of alkoxide is evident in the complexes by both crystallography and ^{1}H NMR, where the methoxide singlet peak occurs between 4.50 and 5.90 ppm and the multiplet attributed to the isopropoxide appears near 5.00 ppm. The presence of small resonances due to free methanol or isopropanol are also evident in the NMR spectra and indicates the lability of the alkoxide ligand in solution. The proton NMR spectrum of [(L10O)WO_2(OPr^i)] is presented in Fig. 1.

Although it is well known that W(VI) dioxo complexes are poorer oxygen atom donors and W(IV) complexes better oxygen atom acceptors, than the corresponding Mo species, we could see no evidence for oxygen atom transfer (OAT) reactivity with our tungsten complexes even under condition more forcing than those that led to facile OAT between the Mo complexes and an acceptor such as triphenylphosphine. Thus while heating [(L)MoO_2Cl] in pyridine with a slight excess of triphenylphosphine for several hours led to isolation of the stable Mo(IV) complex, [(L)MoOCl(py)] and triphenylphosphine oxide, no reaction occurred with the W analogs even after heating for several days.

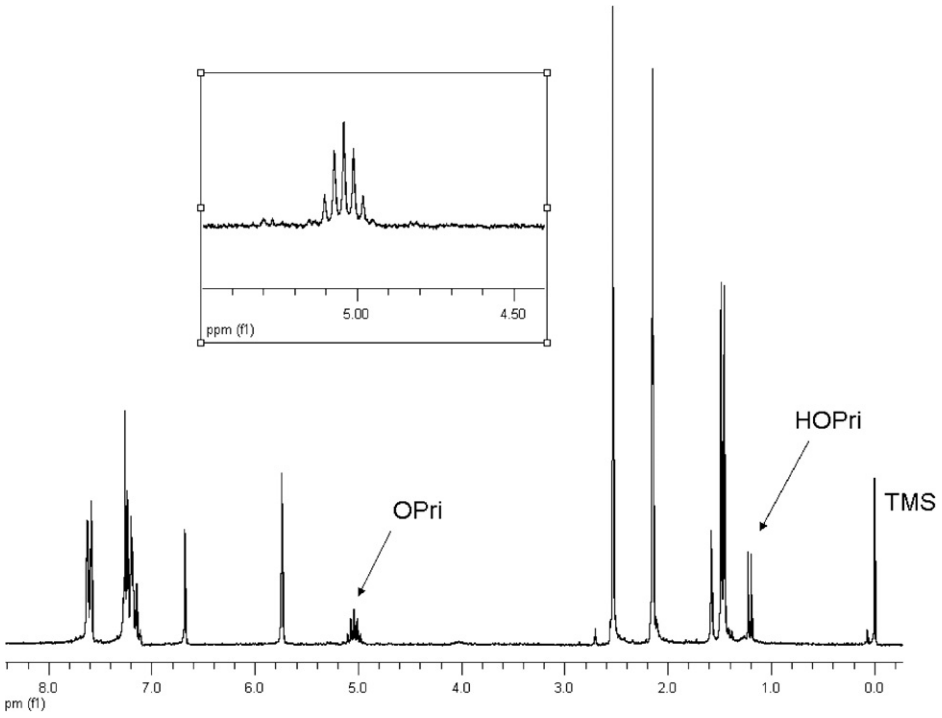

Fig. 1. The ^{1}H NMR spectrum in CD_3Cl shows peaks from [(L10O)WO_2(OPr^i)] (**4**). The arrow indicates both the isopropoxide and free isopropanol.

3.2. Structure

We report here the structure of one chloro, and one alkoxy complex of the type [(L)WO_2X] along with the μ-oxo dimer of the L4O ligand as representative examples.

[(L1O)WO_2Cl]. The structure of the chloro complex of the L1OH ligand shows that in the solid state it is the symmetric *cis* isomer. The molecule displays a crystallographic plane of symmetry passing through the chloro group, the tungsten and the phenolate ring rendering only one half the molecule unique. The most obvious difference between the corresponding molybdenum and tungsten complexes of L1OH relate to the longer bond of W=O (1.788(5) Å) compared to Mo=O (1.710(6) Å). This is likely the result of a small amount of compositional disorder between the chloride and the oxo groups which leads to longer than expected W–O_{oxo} bonds and a shorter than expected W–Cl bond as is commonly seen with these types of complexes. The overall molecular structure of **1** (Fig. 2) is otherwise very similar to the Mo analog and the alkoxy complex **6**, displaying a six-coordinate distorted octahedral geometry with chelation from the two pyrazole nitrogens, an aromatic phenolate, two oxo atoms, and a chloride. The relatively short tungsten W–$O_{phenolate}$ distance of 1.910(6) Å is similar to that seen for the alkoxide in **6** and is indicative of a small amount of multiple bond character.

[(L10O)WO_2(OMe)]. The ORTEP in Fig. 3 shows the distorted octahedral molecular structure of **6** which has approximate C_s symmetry with a noncrystallographic plane passing through O3, W1 and O4. The two pyrazole

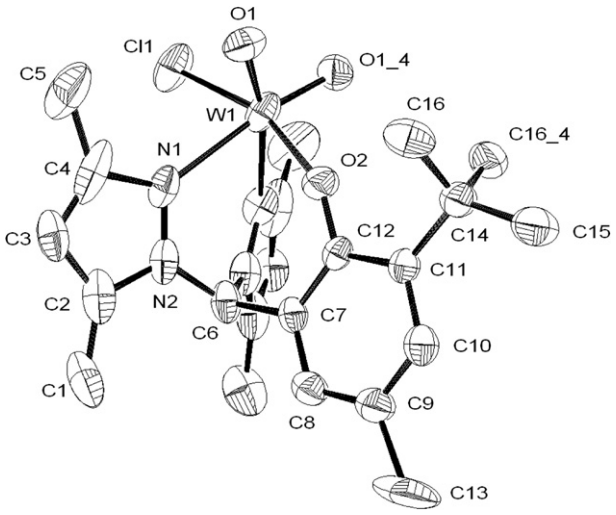

Fig. 2. ORTEP diagram with 50% thermal ellipsoids of [(L1O)WO_2Cl] (**1**) showing partial atomic labeling. Hydrogen atoms have been omitted for clarity.

nitrogens again coordinate in a bidentate planar fashion to the tungsten(VI) center *trans* to the oxo atoms. The nitrogen and oxo donors lie in a pseudoequatorial plane with the alkoxide oxygen from the heteroscorpionate ligand and methoxide oxygen *trans* to each other and occupying the "axial" sites. The W–O_{Me} bond length, found at 1.913 Å is virtually identical that the Mo–O_{Me} in the corresponding Mo complex and is shorter than the Mo–$O_{heteroscorpionate}$ bond *trans* to it by 0.025 Å due to the *trans* effect.

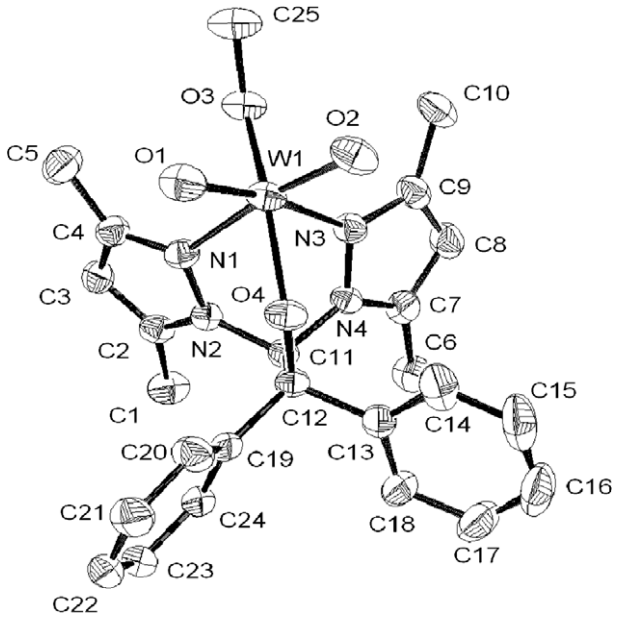

Fig. 3. ORTEP diagram with 50% thermal ellipsoids of [(L10O)WO_2(OMe)] (**6**) showing complete atomic labeling. Hydrogen atoms have been omitted for clarity.

[(L4O)WO_2]$_2$O. Attempts to grow single crystals of [(L4O)WO_2Cl] for structural determination instead yielded the μ-oxo dimer, **12**. Crystals of the μ-oxo dimers are often obtained when the mononuclear complexes remains in solution for an extended time (particularly at room temperature) and the alkoxide complexes appear to be the most susceptible to this process due to the lability of the alkoxide ligand in solution as demonstrated by ^{1}H NMR. The structure of **12** (Fig. 4) reveals two mononuclear dioxo-tungsten units of approximate octahedral geometry bridged by a single oxygen atom. The molecule has approximate, but non-crystallographic, inversional symmetry with two W atoms sharing similar bond lengths and angles. Thus all of the terminal W=O bonds have almost identical bond lengths of approximately 1.71(1) Å, similar to their values in the non-compositionally disordered monomers. The bridging oxygen to tungsten bonds are longer (ca. 1.88 Å) as expected, with the W1–O9–W2 angle slightly bent from linear at 168.2°. Unlike the two monomers the dimer adopts the *trans* geometry where the carboxylate donor of the heteroscorpionate ligand is *trans* to an oxo group. This results in a relatively long W–$O_{carboxyl}$ bonds averaging 2.12 Å due to the strong *trans* effect of the oxo group. It also leads to asymmetric values for the W–$N_{pyrazole}$ bonds with those pyrazole groups *trans* to an oxo atom averaging 2.34 Å (similar to those seen in the *cis* monomers) while those *trans* to the bridging oxygen are about 0.12 Å shorter at 2.21 Å. Unlike the case with all the other heteroscorpionate ligands where the *cis* geometry is the thermodynamically more stable one for these dioxo W(VI) complexes, but similar to that seen in the Mo analogs, the L4O complexes preferentially adopt the *trans* geometry. The origin of this effect is still under investigation.

3.3. Isomerization kinetics

The isomerization of the *trans*-[(L10O)WO_2Cl] isomer to the thermodynamically more stable *cis*-[(L10O)WO_2Cl] was followed by ^{1}H NMR in DMSO-d_6 by measuring the changes in relative intensity of the pyrazole protons as a function of time and temperature (Table 4 and Fig. 5). A similar isomerization process has been demonstrated for

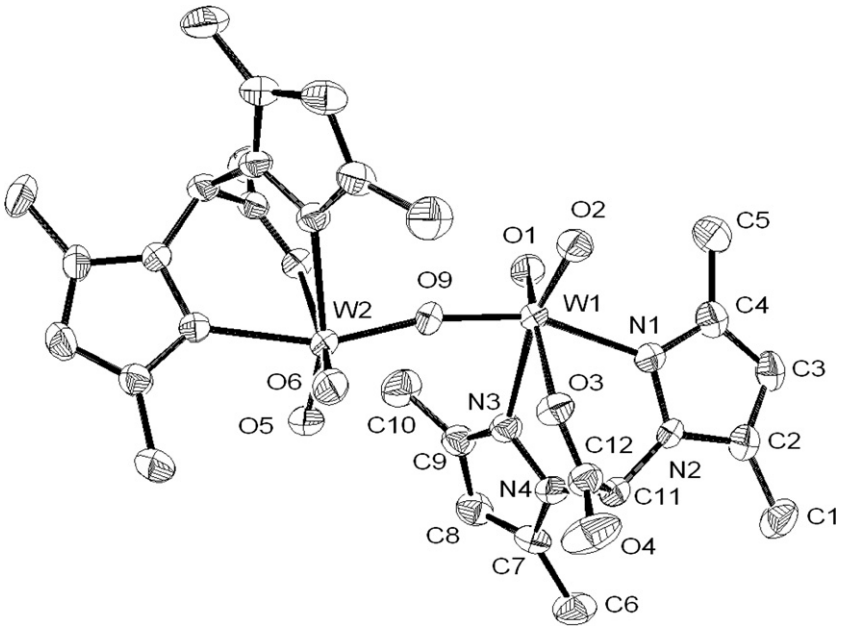

Fig. 4. ORTEP diagram with 50% thermal ellipsoids of [(L4O)WO_2]$_2$O (**12**) showing partial atomic labeling. Hydrogen atoms have been omitted for clarity.

Table 4
Activation parameters and first-order rate constants for the isomerization of [(L10O)WO_2Cl]

Temperature (K)	k (s^{-1})
318	1.84×10^{-5}
323	3.30×10^{-5}
328	4.85×10^{-5}
333	6.35×10^{-5}
$\Delta H^{\ddagger}$ (kcal/mol)	17
$\Delta S^{\ddagger}$ (cal/K mol)	−28

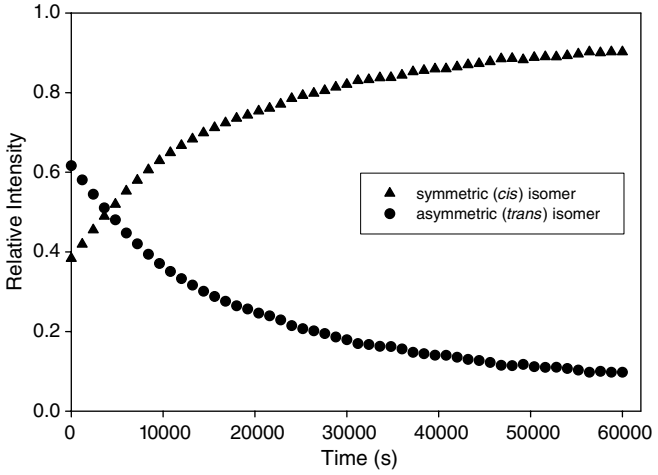

Fig. 5. The above plot shows the asymmetric (*trans*) complex transforming to the thermodynamic symmetric (*cis*) product at 60 °C in DMSO-d_6.

both Mo(VI) and Mo(V) complexes of L10OH and L1OH, allowing for a direct comparison with the analogous W(VI) species. In the case of the isomerization of the dioxo Mo(VI) complex [(L10O)MoO_2Cl], the kinetically formed isomer is the *trans*, which isomerizes to the more stable *cis* with a first-order rate constant at 60 °C of $2.9(3) \times 10^{-4}$ s^{-1}. For [(L10O)WO_2Cl] the *trans* isomer is again the kinetically formed one, which isomerizes to the more stable *cis* isomer. However the rate constant for the isomerization of the tungsten complex at the same temperature is determined here to be $6.3(13) \times 10^{-5}$ s^{-1}; nearly five times slower than its Mo(VI) counterpart [30]. Thermodynamic parameters determined from the Erying equation gave values $\Delta H^{\ddagger} = 17$ kcal/mol and $\Delta S^{\ddagger} = -28$ eu. These differ from those seen for the analogous Mo(VI) complex of $\Delta H^{\ddagger} = 19$ kcal/mol and $\Delta S^{\ddagger} = -17$ eu. The difference in isomerization rate between Mo and W is clearly the result of entropic rather than enthalpic effects since $\Delta\Delta H^{\ddagger}$ between W and Mo is essentially zero while $\Delta\Delta S^{\ddagger}$ is an unfavorable by over 10 eu. Although the magnitude of the entropy of activation is still probably too small to definitely assign any mechanism, the significantly more negative entropy of activation is suggestive of an isomerization pathway for W that leads to a more ordered transition state than that seen for the Mo analog where the preponderance of the evidence is consistent with a trigonal-twist mechanism [30].

3.4. Conclusions

Twelve new dioxo W(VI) complexes of a family heteroscorpionate ligands of the type [(L)WO_2Y], where L = N_2X ligand and Y = Cl, OMe or OPr^i, have been synthesized and characterized. The alkoxy groups in these complexes are kinetically labile as determined by NMR and the isolation of μ-oxo dimers rather than the mononuclear complexes during attempts at crystallization at room temperature. With the more sterically bulky heteroscorpionate ligands both *cis* and *trans* geometrical isomers can be isolated, the tungsten complexes of which isomerize five times slower than the Mo analogs.

Acknowledgements

This work was supported in part by Grant CHE-0313865 from the NSF. The NSF-MRI program Grant CHE-0320848 is acknowledged for support of the X-ray diffraction facilities at San Diego State University.

Appendix A. Supplementary material

CCDC 620363, 620363 and 620365 contains the supplementary crystallographic data for **1**, **6** and **12**. These data can be obtained free of charge via http://www.ccdc.cam.ac.uk/conts/retrieving.html, or from the Cambridge Crystallographic Data Centre, 12 Union Road, Cambridge CB2 1EZ, UK; fax: (+44) 1223-336-033; or e-mail: deposit@ccdc.cam.ac.uk. Supplementary data associated with this article can be found, in the online version, at doi:10.1016/j.ica.2006.10.024.

References

[1] M.M. Abu-Omar, Chem. Commun. (2003) 2102.
[2] J.H. Enemark, J.J. Cooney, J. Wang, R.H. Holm, Chem. Rev. 104 (2004) 1175.
[3] R. Hille, Chem. Rev. 96 (1996) 2757.
[4] Z.Z. Xiao, C.G. Young, J.H. Enemark, A.G. Wedd, J. Am. Chem. Soc. 114 (1992) 9194.
[5] L.J. Laughlin, C.G. Young, Inorg. Chem. 35 (1996) 1050.
[6] P.D. Smith, A.J. Millar, C.G. Young, A. Ghosh, P. Basu, J. Am. Chem. Soc. 122 (2000) 9298.
[7] V.N. Nemykin, S.R. Davie, S. Mondal, N. Rubie, A. Somogyi, M.L. Kirk, P. Basu, J. Am. Chem. Soc. 124 (2002) 756.
[8] F.E. Inscore, R. McNaughton, B.L. Westcott, M.E. Helton, R. Jones, I.K. Dhawan, J.H. Enemark, M.L. Kirk, Inorg. Chem. 38 (1999) 1401.
[9] S.B. Seymore, S.N. Brown, Inorg. Chem. 39 (2000) 325.
[10] S. Thomas, A.A. Eagle, A.S. Sproules, J.P. Hill, J.M. White, E.R.T. Tiekink, G.N. George, C.G. Young, Inorg. Chem. 42 (2003) 5909.
[11] A.A. Eagle, E.R.T. Tiekink, C.G. Young, Inorg. Chem. 36 (1997) 6315.
[12] A.A. Eagle, G.N. George, E.R.T. Tiekink, C.G. Young, Inorg. Chem. 36 (1997) 472.
[13] B.S. Hammes, C.J. Carrano, Inorg. Chem. 38 (1999) 666.
[14] B.S. Hammes, C.J. Carrano, J. Chem. Soc., Dalton Trans. (2000) 3304.
[15] A. Otero, J. Fernandez-Baeza, A. Antinolo, J. Tejeda, A. Lara-Sanchez, J. Chem. Soc., Dalton Trans. (2004) 1499.

[16] S.R. Davie, N. Rubie, B.S. Hammes, C.J. Carrano, M.L. Kirk, P. Basu, Inorg. Chem. 40 (2001) 2632.
[17] B. Kail, V.N. Nemykin, S.R. Davie, C.J. Carrano, B.S. Hammes, P. Basu, Inorg. Chem. 41 (2002) 1281.
[18] B.S. Hammes, B.S. Chohan, J.T. Hoffman, S. Einwächter, C.J. Carrano, Inorg. Chem. 43 (2004) 7800.
[19] G.N. George, J.A. Mertens, W.H. Campbell, J. Am. Chem. Soc. 121 (1999) 9730.
[20] K. Heffron, C. Leger, R.A. Rothery, J.H. Weiner, F.A. Armstrong, Biochemistry 40 (2001) 3117.
[21] K. Peariso, B.S. Chohan, C.J. Carrano, M.L. Kirk, Inorg. Chem. 42 (2003) 6194.
[22] (a) L.D. McPherson, M. Drees, S.I. Khan, T. Straaner, M.M. Abu-Omar, Inorg. Chem. 43 (2004) 4036;
(b) D.W. Lahti, J.H. Espenson, J. Am. Chem. Soc. 123 (2001) 6014;
(c) J. Jung, T.A. Albright, D.M. Hoffman, Lee T. Randall, Dalton Trans. (1999) 4487.
[23] H. Oku, N. Ueyama, M. Kondo, A. Nakamura, Inorg. Chem. 33 (1994) 209.
[24] (a) A. Otero, J. Fernández-Baeza, F. Carrillo-Hermosilla, J. Tejeda, A. Lara-Sánchez, M. Fernández-López, A.M. Rodríguez, I. López-Solera, Inorg. Chem. 41 (2002) 5193;
(b) J.T. Hoffman, S. Einwächter, B.S. Chohan, P. Basu, C.J. Carrano, Inorg. Chem. 43 (2004) 7573.
[25] S. Yu, R.H. Holm, Inorg. Chem. 28 (1989) 4385.
[26] V.C. Gibson, T.P. Kee, A. Shaw, Polyhedron 7 (1988) 579.
[27] (a) Y.L. Wong, Y. Yan, E.S. Chan, Q. Yang, T.C.W. Mak, D.K.P. Ng, J. Chem. Soc., Dalton Trans. (1998) 3057;
(b) Y.L. Wong, J.F. Ma, W.F. Law, Y. Yan, W.T. Wong, Z.Y. Zhang, T.C.W. Mak, D.K.P. Ng, Eur. J. Inorg. Chem. (1999) 313;
(c) Y.L. Wong, J.F. Ma, F. Xue, T.C.W. Mak, D.K.P. Ng, Organometallics 18 (1999) 5075.
[28] K. Dreisch, C. Andersson, C. Stalhandske, Polyhedron 10 (1991) 2417.
[29] A. Lehtonen, R. Sillanpää, Inorg. Chem. 43 (2004) 6501.
[30] J.T. Hoffman, B.L. Tran, C.J. Carrano, J. Chem. Soc., Dalton Trans. (2006) 3822.